Applied Energy 87 (2010) 592–598

Contents lists available at ScienceDirect

Applied Energy

journal homepage: www.elsevier.com/locate/apenergy

Size optimization of a PV/wind hybrid energy conversion system with battery storage using simulated annealing

Orhan Ekren [a], Banu Y. Ekren [b,*]

[a] Ege University, Department of HVAC, Ege Vocational Training School, Bornova, Izmir 35100, Turkey
[b] Pamukkale University, Department of Industrial Engineering, Kinikli, Denizli 20070, Turkey

ARTICLE INFO

Article history:
Received 30 January 2009
Received in revised form 12 March 2009
Accepted 16 May 2009
Available online 30 June 2009

Keywords:
Hybrid energy
Optimization
Simulation
Simulated annealing

ABSTRACT

In this paper, we perform Simulated Annealing (SA) algorithm for optimizing size of a PV/wind integrated hybrid energy system with battery storage. The proposed methodology is a heuristic approach which uses a stochastic gradient search for the global optimization. In the study, the objective function is the minimization of the hybrid energy system total cost. And the decision variables are PV size, wind turbine rotor swept area and the battery capacity. The optimum result obtained by SA algorithm is compared with our former study's result. Consequently, it is come up with that the SA algorithm gives better result than the Response Surface Methodology (RSM). The case study is realized for a campus area in Turkey.

1. Introduction

Alternative energy sources such as solar and wind energies, has attracted many researchers and communities throughout the world since the "energy crisis" of the 1970s [1]. In addition, the increasing energy demand, high energy prices, as well as increasing concerns over environmental-, health- and climate changed implications of energy related activities are increasing concerns on alternative energy studies in communities [2–11].

The high costs of electricity may be due to centralized energy systems which operate mostly on fossil fuels and require large investments for establishing transmission and distribution grids that can penetrate remote regions [12]. Furthermore, the fossil fuel combustion results in the emission of obnoxious gases rising concerns about the climate change and other health hazards.

In order to counter these problems there is a strong need for alternative systems of power generation and distribution. Unlike the centralized energy systems, on the other hand, decentralized energy systems are mostly based on renewable energy sources. They operate at lower scales (a few kW h scale) both in the presence and absence of grid, and easily accessible to remote locations because of generation of power in the propinquity of demand site.

Stand-alone systems produce power independently of the utility grid; hence, they are said to stand-alone. These are more suitable for remotest locations where the grid cannot penetrate and there is no other source of energy. These systems are not connected to the utility grid as a result they need batteries for storage of electricity produced during off-peak demand periods, leading to extra battery and storage costs.

It is prudent that neither a standalone solar nor a wind energy system can provide a continuous supply of energy due to seasonal and periodical variations. Therefore, in order to satisfy the continuous load demand in remote locations, hybrid energy systems are implemented on combined solar and wind energy conversion units with battery storage. A great deal of research [13–24] has been carried out on hybrid energy systems with respect to performance and optimization. However, most of them use historical data and/or intervals for the input, wind/solar energy, electricity demand, variables of the system. In this study, we utilize probabilistic distributions in order to carry out random input simulation for the hybrid system. We implement a case study to model a stand-alone hybrid energy system at a remote location from the grid system. The system is modeled to meet electricity demand of a global system for mobile communications (GSM) base station on a campus area, in Turkey.

A schematic diagram of a basic hybrid energy system is given in Fig. 1. As seen in figure, the electricity produced via PV array and wind turbine is regulated by voltage regulator components and the excess electricity produced by the hybrid system is stored by the battery banks to be used for later lacking loads. Here, the amount of the electricity produced via the wind and the solar energy depends on the total solar radiation on horizontal surface and the wind speed in general.

* Corresponding author. Tel.: +90 258 295 3132; fax: +90 258 295 3262.
E-mail address: byekren@pamukkale.edu.tr (B.Y. Ekren).

0306-2619/$ - see front matter © 2009 Elsevier Ltd. All rights reserved.
doi:10.1016/j.apenergy.2009.05.022

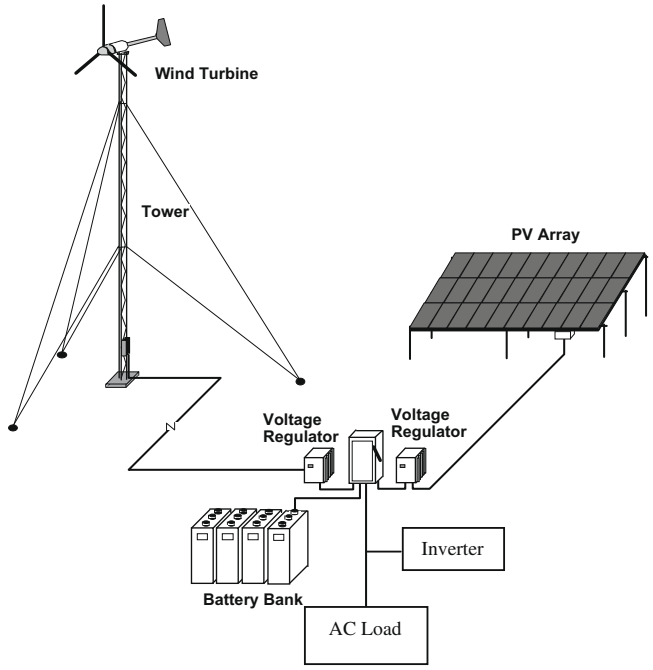

Fig. 1. Schematic diagram of a basic hybrid energy system.

2. Background and motivation

Hybrid energy systems are usually more reliable and less costly than the systems that use a single source of energy [19]. However, the mathematical modeling and sizing and control of the hybrid system require a significant number of variables [25]. Classic optimization techniques are not able to capture various design alternatives so do not give good results. Therefore, other techniques that allow satisfactory results are required. Evolutionary algorithms [26–28] are known with the advantage of having low computational requirements, thus obtaining good solutions at a reasonable time.

The only available design tool capable of carrying out the design of this type of hybrid system is HOMER [29]. This tool uses an enumerative method to obtain the optimal design by evaluating all the possible solutions. However, when the number of possible design points is very high, the enumerative method requires excessively high calculation time. Size optimization of a hybrid energy system is a continuous type optimization problem. Therefore, this property also increases the possible design points of decision variables, drastically. Thus, we propose utilizing heuristic techniques, such as the evolutionary algorithms, to solve these kinds of optimization problems. Heuristic techniques allow us to obtain good solutions using a reasonable CPU effort. The evolutionary algorithms have been applied successfully to solve many problems of design in engineering [30,31]. Another design tool, HOGA, is developed by Bernal-Agustín and Dufo-López [28] which uses an evolutionary algorithm for the design of hybrid systems. HOGA is capable of applying an enumerative algorithm and useful for validating the results reached by means of the evolutionary algorithm. Yang et al. [17] also completes the optimization procedure of a hybrid energy system using genetic algorithm.

We are motivated by the usefulness of the evolutionary algorithms in solving such time-consuming optimization systems. In this paper, our aim is to solve the hybrid system problem using a different evolutionary algorithm, SA. SA's major advantage over other methods is an ability to avoid becoming trapped in local minima. The algorithm employs a random search which not only accepts changes that decrease the objective function (assuming a minimization problem), but also some changes that increase it. The other objective of this study is to compare the SA results with our former study's RSM results [32,33]. The simulation and optimization procedure are completed using ARENA 12.0, a commercial simulation software.

3. PV/wind hybrid energy system simulation

The hybrid system relies on solar and wind energies as the primary power resources, and it is backed up by the batteries (see Fig. 1). Here, batteries are used due to the stochastic characteristics of the system inputs, solar radiation, wind speed, and the electricity consumption of the place. The potential energy resources such as solar and wind energy sources are not controllable variables and the behavior of these variables are non-deterministic. Therefore, probability distributions are specified in order to carry out a random-input simulation. Hourly solar radiation's and wind speed's theoretical distributions are fitted to a suitable distribution using ARENA 12.0 input analyzer based on historical data [34]. In the simulation model hourly data are used so, one of the hybrid system's simulation model assumptions is that the input variables do not change throughout an hour. The length of each simulation run is considered as twenty years of the economical life which consists of 365 days/year, 24 h/day, in total 175,200 h. For each run, 10 independent replications are completed. In the simulation model, since it is a popular and useful variance reduction technique to compare two or more alternative configurations, the common random numbers (CRN) variance reduction technique is used. And because a steady state analysis is needed to analyze a long time period, the warm-up period is decided as 17,000 h [35].

Table 1
Main characteristics of the meteorological station.

Instrument	Specification/description		
Pyranometer (CM11)	Wieving angle: 2π Irradiance: 0–1400 W/m^2 Sensitive: $5.11 * 10^{-6}$ V per W/m^2 (±0.5% at 20 °C and 500 W/m^2) Expected signal output: 0–10 mV Response time for 95% response: <15 sec.		
Data logger	Module capacity:192,896 bytes 12 Signal inputs		
	Measurement range	Recording resolution	Accuracy
Anemometer (for speed)	0.3–50 m/s	⩽0.1 m/s	± 0.3 m/s
Wind vane (for direction)	0°–360°	⩽1°	±2°
Thermometer	(−30) to (+70) °C	⩽0.1 °C	±0.2 K
Hygrometer	0–100% RH	1% RH	±2% RH
Barometer	800–1600 kPa	⩽1 kPa	–

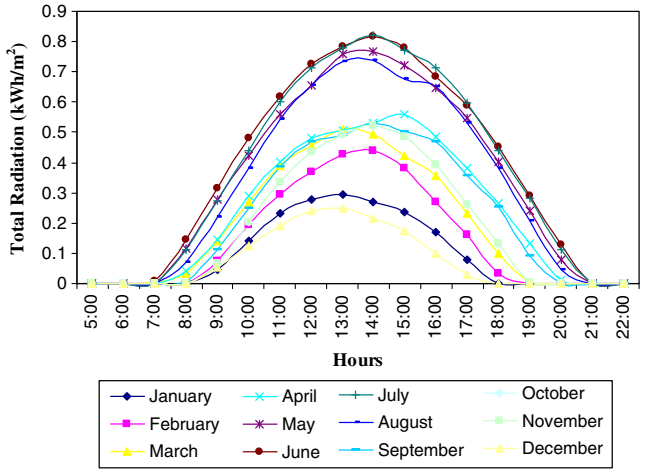

Fig. 2. Average hourly total solar radiation on horizontal surface (measured).

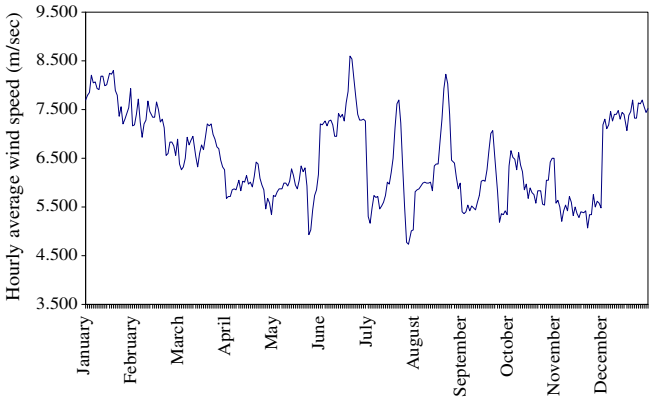

Fig. 3. Average hourly average wind speeds (measured).

Hourly mean solar radiation and wind speed data for the period of 2001–2003 are recorded at a meteorological station where the suggested hybrid energy system is to be established [36]. Technical specifications of the meteorological station are given in Table 1.

3.1. Solar radiation

Fig. 2 shows the measured hourly total solar radiation on horizontal surface, *H*, based on months in a year. From figure, it can be obtained that the most efficient months and hours in utilizing solar energy are in June, July and August, between 11.00 and 16.00. Hourly total solar radiation on tilted surface, I_T, is calculated using *H* [37] and optimum tilted angle of the PV panel, β is taken as 38°.

Table 2 presents fitted hourly total solar radiation distributions, for example, for three months, June, July, and August. In this table, solar radiations have different distributions at each hour of the months. This means that solar radiation may have different values in accordance with its distribution at each hour of the months which is not known in advance, except the zero values. Here, zero values are at the morning and evening hours, due to the sunset.

Arena simulation software uses nine different theoretical distributions to fit data to a theoretical distribution. These are, Exponential, Gamma, Lognormal, Normal, Triangular, Uniform, Weibull, Erlang, and Beta distributions. Each of them has its own probabilistic characteristics in creating random variables in a stochastic model.

3.2. Wind speed

In order to measure wind speed and prevailing wind direction, a three-cup anemometer and a wind vane are used. The measured hourly average wind speeds at 10-m-height for all months of the year can be seen in Fig. 3. Table 3 shows hourly wind speed distributions of 3 months as an example.

3.3. Electricity consumption

The third stochastic data is the electricity consumption of the GSM base station. The data are collected from a base station on campus area for every hour of the day. In this study, the existence of a seasonal effect on the GSM base station's electricity consumption is ignored. The statistical data are collected in 15 random days in each season, fall, winter, spring, and summer. Hence, totally

Table 2
Hourly solar radiation on horizontal surface distributions for months June, July, and August (W/m2).

Hours	Months		
	June	July	August
00:00–01:00	0	0	0
01:00–02:00	0	0	0
02:00–03:00	0	0	0
03:00–04:00	0	0	0
04:00–05:00	0	0	0
05:00–06:00	0	0	0
06:00–07:00	−0.001 + 37 * BETA(0.0269, 0.0857)	0	0
07:00–08:00	48 + 123 * BETA(2.71, 0.787)	NORM(113, 12.9)	18 + 80 * BETA(2.22, 1.22)
08:00–09:00	NORM(313, 16.6)	TRIA(240, 278, 305)	80 + 189 * BETA(3.49, 1.22)
09:00–10:00	NORM(482, 19.9)	270 + 209 * BETA(3.26, 0.724)	183 + 246 * BETA(1.57, 0.542)
10:00–11:00	481 + 173 * BETA(2.39, 0.602)	NORM(602, 17.2)	NORM(545, 55.8)
11:00–12:00	558 + 206 * BETA(2.51, 0.601)	NORM(714, 28.1)	265 + 457 * BETA(2.76, 0.465)
12:00–13:00	538 + 297 * BETA(1.34, 0.431)	517 + 337 * BETA(3.95, 1.11)	221 + 617 * BETA(3.05, 0.62)
13:00–14:00	472 + 399 * BETA(1.5, 0.42)	672 + 187 * BETA(3.27, 0.858)	145 + 704 * BETA(2.09, 0.385)
14:00–15:00	229 + 617 * BETA(1.13, 0.313)	400 + 436 * BETA(1.32, 0.415)	144 + 655 * BETA(0.978, 0.366)
15:00–16:00	359 + 411 * BETA(1.02, 0.402)	453 + 311 * BETA(0.931, 0.405)	334 + 393 * BETA(1.45, 0.507)
16:00–17:00	198 + 450 * BETA(1.09, 0.303)	174 + 481 * BETA(1.34, 0.407)	193 + 464 * BETA(2.78, 1.04)
17:00–18:00	178 + 326 * BETA(1.28, 0.418)	46 + 452 * BETA(1.16, 0.347)	76 + 371 * BETA(1.47, 0.483)
19:00–20:00	103 + 233 * BETA(1.55, 0.387)	69 + 258 * BETA(2.46, 0.527)	TRIA(78, 266, 278)
20:00–21:00	63 + 91 * BETA(1.54, 0.604)	−0.001 + 148 * BETA(3.43, 1.02)	−0.001 + 101 * BETA(0.974, 1.13)
22:00–23:00	0	0	0
23:00–00:00	0	0	0

Table 3
Hourly average wind speed distributions for months, January, February, and March (m/sec).

Hours	Months		
	January	February	March
00:00–01:00	TRIA(2, 3.08, 18)	2 + 13 * BETA(1.07, 1.57)	1 + 12 * BETA(1.46, 1.79)
01:00–02:00	1 + LOGN(7.02, 5.28)	WEIB(7.75, 1.88)	1 + 11 * BETA(1.54, 1.66)
02:00–03:00	2 + 14 * BETA(0.881, 1.23)	GAMM(2.24, 3.31)	TRIA(2, 3.95, 13)
03:00–04:00	NORM(8.22, 3.96)	1 + LOGN(7.1, 5.85)	TRIA(1, 4.52, 14)
04:00–05:00	2 + WEIB(6.7, 1.52)	1 + LOGN(6.61, 5.58)	NORM(6.93, 2.66)
05:00–06:00	TRIA(2, 4.21, 18)	1 + LOGN(6.3, 5.69)	2 + WEIB(5.3, 1.78)
06:00–07:00	1 + 15 * BETA(1.37, 1.6)	2 + WEIB(5.5, 1.2)	TRIA(1, 7.62, 12)
07:00–08:00	1 + LOGN(7.23, 5.21)	2 + WEIB(5.87, 1.48)	TRIA(1, 7, 13)
08:00–09:00	2 + WEIB(6.84, 1.66)	2 + 17 * BETA(1.14, 2.28)	TRIA(1, 7.69, 10.9)
09:00–10:00	1 + WEIB(8.11, 2.12)	2 + WEIB(5.98, 1.41)	1 + GAMM(1.13, 4.69)
10:00–11:00	2 + WEIB(6.71, 1.8)	1 + WEIB(7.1, 1.61)	2 + WEIB(5.15, 2.25)
11:00–12:00	2 + WEIB(6.78, 1.87)	1 + ERLA(2.11, 3)	NORM(6.77, 2.54)
12:00–13:00	3 + ERLA(2.63, 2)	2 + 22 * BETA(0.955, 2.76)	NORM(6.68, 2.81)
13:00–14:00	2 + GAMM(2.45, 2.54)	1 + WEIB(7.24, 1.56)	1 + ERLA(1.98, 3)
14:00–15:00	2 + WEIB(6.97, 1.58)	1 + WEIB(6.92, 1.57)	1 + WEIB(6.97, 1.76)
15:00–16:00	2 + WEIB(6.54, 1.6)	1 + WEIB(7.06, 1.61)	NORM(7.17, 3.63)
16:00–17:00	2 + WEIB(6.41, 1.63)	1 + WEIB(6.86, 1.6)	2 + 17 * BETA(1.37, 3.1)
17:00–18:00	NORM(7.35, 3.12)	1 + ERLA(2.8, 2)	NORM(6.98, 2.9)
19:00–20:00	TRIA(2, 4.7, 16)	NORM(6.84, 3.82)	1 + LOGN(6.07, 3.79)
20:00–21:00	2 + WEIB(5.76, 1.57)	1 + WEIB(6.46, 1.57)	2 + 12 * BETA(1.06, 1.56)
22:00–23:00	1 + WEIB(7.01, 1.73)	1 + WEIB(6.4, 1.62)	1 + GAMM(1.84, 3.1)
23:00–00:00	NORM(7.41, 4.06)	1 + WEIB(6.4, 1.62)	TRIA(2, 4.39, 13)

$15 * 4 = 60$ electricity consumption data are collected for an hour (e.g., for 1.00 pm). Then these data are fitted to theoretical distributions without considering seasonal effects. Fig. 4 illustrates the hourly mean electricity consumption values of the GSM base station. And the fitted distributions are given in Table 4.

3.4. Formulations

If the hybrid energy systems are well designed, they provide a reliable service for an extended period of time. The sizes of system components are decision variables, and their costs are objective function. Objective function here in is the total cost of PV, wind turbine rotor, battery and also the battery charger, installation, maintenance, and engineering cost. A solar and wind hybrid energy system with the sizes of a_s and a_w, respectively, can be defined as:

$$a_s = \eta \cdot A_s \tag{1}$$

where η is the PV module efficiency, A_s is the PV array area and:

$$a_w = C_p \cdot (\pi \cdot r^2) \tag{2}$$

where C_p is the power coefficient, and r is the rotor radius. Here, $\pi \cdot r^2$ represents A_w, rotor swept area. η value is taken as a variable value depending on PV module type and module temperature. In the study, mono-crystal silicon PV module type, rated output of 75 W at 1000 W/m^2 is used. Because in this study we compare two methodologies' results we stick to the same hybrid system assumptions with our former study [32,33]. Here, η value changes between 7% and 17% based on module surface temperatures which are between 10 °C and 70 °C [38,39]. In the simulation model, for December, January and February the temperature and the η values are assumed to be 10 °C and 17%, respectively. For March, April and May the temperature and the η values are assumed to be 50 °C and 10%, respectively. For June, July, August the temperature and the η values are assumed to be 70 °C and 7%, respectively. And, for September, October, November the temperature and the η values are assumed to be 30 °C and 13%, respectively. These values are obtained from a manufacturer firm. C_p value is also taken from a manufacturer firm as a graphic value which changes according to the wind speed value (see Fig. 5).

Wind energy density, W, is calculated by:

$$W = 1/2 \cdot \rho \cdot V^3 \cdot D \tag{3}$$

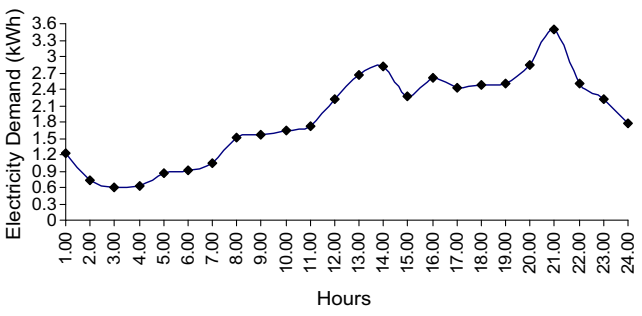

Fig. 4. Hourly average demand of GSM base station.

Table 4
Hourly electricity demands (kW).

Hours	Demands
00:00–01:00	NORM(1.21, 0.602)
01:00–02:00	1.72 * BETA(1.13, 1.55)
02:00–03:00	WEIB(0.645, 1.28)
03:00–04:00	GAMM(0.565, 1.11)
04:00–05:00	EXPO(0.854)
05:00–06:00	3.31 * BETA(1.28, 3.34)
06:00–07:00	2.86 * BETA(1.15, 1.96)
07:00–08:00	WEIB(1.7, 2.36)
08:00–09:00	TRIA(0, 0.827, 3.84)
09:00–10:00	3.84 * BETA(2.46, 3.25)
10:00–11:00	0.15 + 3.34 * BETA(2.54, 2.87)
11:00–12:00	0.28 + LOGN(1.91, 0.951)
12:00–13:00	1 + ERLA(0.828, 2)
13:00–14:00	1 + LOGN(1.82, 1.43)
14:00–15:00	NORM(2.27, 0.626)
15:00–16:00	1 + GAMM(0.669, 2.4)
16:00–17:00	1 + GAMM(0.417, 3.45)
17:00–18:00	NORM(2.47, 0.685)
19:00–20:00	1 + ERLA(0.377, 4)
20:00–21:00	1.11 + ERLA(0.436, 4)
22:00–23:00	1.29 + LOGN(2.2, 1.59)
23:00–00:00	1 + GAMM(0.435, 3.48)

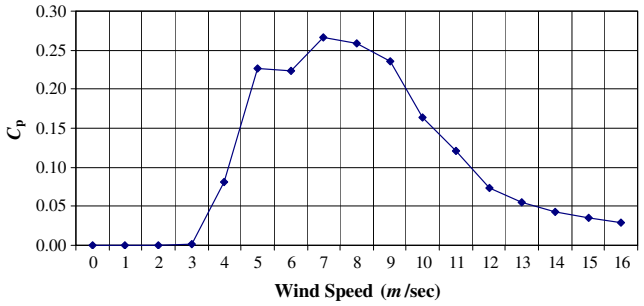

Fig. 5. C_p value versus wind speed.

D is length of period. Because of hourly operating state, it is taken as 1 h. ρ is air density which is considered as 1.225, and V is hourly average wind velocity whose distribution is shown in Table 3.

Solar radiation on tilted plate is calculated for isotropic sky assumption and using equation below:

$$I_T = I_b R_B + I_d(1+\cos\beta)/2 + (I_b + I_d)\rho(1-\cos\beta)/2 \quad (4a)$$

$$R_b = \cos\theta/\cos\theta z \quad (4b)$$

where I_T is the total solar radiation on tilted surface, I_b the horizontal beam radiation, I_d the horizontal diffuse radiation, R_b the ratio of beam radiation on tilt factor, θ the incidence angle, θz the zenith angle, and ρ is the surface reflectivity, β is tilted angle of the plate.

The supply of hourly solar and wind energies must meet the hourly demand, d. This expression can be formulated as:

$$S \cdot a_s + W \cdot a_w \geq d \quad (5)$$

where S is the solar energy density on tilted surface, H_T (kW h/m^2) and W is the wind energy density (kW h/m^2). If Eq. (4b) is not realized, stored energy in the battery will be used. The battery is considered as full in the simulation initially and its efficiency is assumed as 85%. The inverter's efficiency is considered 90% here. If the total of solar, wind, and battery energies still cannot meet the demand, the energy shortage will be supplied by an auxiliary energy source, whose unit cost, herein, is considered \$0.5 per kW h electricity. In this study, the location of the hybrid system is assumed in such a place where the unit cost of the auxiliary energy is more expensive than the electricity produced by the hybrid system. Therefore, the cost of extra energy here is decided such that it is three times as much of the average unit cost of the electricity produced by the hybrid system. Otherwise, if the unit cost of the auxiliary energy was less than that of the electricity produced by the hybrid system, the shortage could be supplied from the auxiliary energy source all the time without the need for such a hybrid system [18]. As seen in Eq. (5), the auxiliary energy cost is also a part of the total hybrid system cost. C_s, C_w, C_B, C_{sh} and C_T are the unit cost of photovoltaic, wind energy generator, battery, shortage electricity, and total hybrid energy system, respectively. B_C denotes the battery capacity. E_i is the total amount of the electricity energy shortage because of not meeting the demand during an hour i. C_s are \$5.8/W_p (mono-crystal silicon, rated output of 75 W at 1000 W/m^2), whereas C_w is US \$3/W (rated output of 5000 W at 10 m/s), and C_B is \$180/kW h (200 Ah 12 V lead acid battery) [14]. C_{sh} is \$0.5 per kW h as explained above, and n is the simulation time period, 175,200 h. In this study, the inflation rate and time value of money are not considered.

$$C_T = C_s \cdot a_s + C_w \cdot a_w + C_B \cdot B_C + \sum_{i=1}^{n} C_{sh} \cdot E_i \quad (6)$$

In addition, a total of US \$500 battery charger cost, and 5% installation, maintenance and engineering cost of the initial hardware is also added into the total system cost for an assumed 20-year-lifetime.

4. Simulated annealing algorithm and solution

SA was first introduced as an intriguing technique for optimizing functions of various variables [40]. It is a heuristic strategy that provides a means for optimization of NP-complete problems for which an exponentially number of steps is required to generate an exact answer. Although such a heuristic approach cannot guarantee to produce the exact optimum, it is known that an acceptable optimum can be found in a reasonable time [41]. Heuristic approaches are most often applied to computationally intractable NP-hard problems because solving these problems exactly can take an exponential amount of computation time, like in our problem. SA is based on an analogy to the cooling of heated metals. The basic algorithm of SA may be described as follows: Successively, a candidate move is randomly selected; this move is accepted if it leads to a solution with a better objective function value than the current solution. Otherwise the move is accepted with a probability that depends on the deterioration Δf of the objective function value. The probability of acceptance is usually computed as $e^{\frac{-\Delta f}{t}}$, using a temperature t as control parameter and $\Delta f = f(y) - f(x)$. This temperature t is gradually reduced according to some cooling schedule, so that the probability of accepting deteriorating moves decreases in the course of the annealing process. From a theoretical point of view, a SA process may converge to an optimal solution if some conditions are met for instance, with an appropriate cooling schedule and a neighborhood which leads to a connected solution space [42,43]. Because convergence rates are usually too slow, in practice one typically applies some faster cooling schedule.

The most important advantage of the SA algorithm compared to the conventional local search-based heuristic methods is that the SA is capable of escaping from being trapped into a local optimum by accepting, in small probability, worse solutions during its iterations. The algorithm employs a random search which not only accepts changes that decrease the objective function f (assuming a minimization problem), but also some changes that increase it. To start with, the probability of accepting worse solutions is reasonably high and new candidate solutions are selected from a relatively large set. During the search process, the probability is decreased and the set is reduced. In this way, the search first emphasizes a global and after that a local search. Suppose that we have the current iteration point $x \in R^n$. The next candidate solution y is generated by:

$$y_i = x_i + q \times d_i \quad (7)$$

where q is a uniformly distributed random number from $[-1, 1]$ and $d \in R^n$ is a search direction. Here i shows the decision variable type. The point y is accepted as the next iteration point if it is better than the current iteration point, in other words, $f(y_i) < f(x_i)$ or if it is worse than the current iteration point then, Metropolis [43] criterion is valid:

$$e^{-\left(\frac{f(y_i)-f(x_i)}{t}\right)} > p \quad (8)$$

where p is a uniformly distributed random number from [0, 1]. If Eq. (7) is ensured then the worse candidate is accepted. Here, the parameter $t > 0$ is a so-called temperature and it is decreased during the algorithm.

The basic formulations of simulated annealing do not specifically consider the choice of d. In the implementation used, the length of the search direction d is adjusted component wise so that about a half of the candidate solutions are accepted. The goal of this so-called adaptive adjustment is to sample the function values widely. If more than 60% of the candidates are accepted, then the length of d is extended. For a given temperature, this increases the number of rejections and decreases the percentage of acceptances. On the other hand, if the ratio of acceptance is

less than 40%, then the length of d is correspondingly decreased [44].

In the SA algorithm first, initial parameters are set, e.g., starting point x_i, search direction d, initial temperature $t > 0$, temperature reduction factor $r_t \in (0, 1)$, final accuracy tolerance $\varepsilon > 0$, number of function values used in termination criteria N_ε, number of cycles before search direction adjustment N_s, number of iterations before temperature reduction N_t. Then the iterative procedure starts.

After N_t times through the N_s loops, the temperature, t, is reduced. The new temperature is given by:

$$t = r_t \times t \tag{9}$$

The size optimization problem of the hybrid system is a continuous type problem rather than a discrete type. Therefore, we employ the implementation of simulated annealing described in [44]. This implementation has been found to be robust and easy to use as well as applicable to even complex continuous problems. As a result the initial parameters are set to; $x_1 = 10$, $x_2 = 50$, $x_3 = 60$, $d = 1$, $t = 50{,}000$; $r_t = 0.85$; $\varepsilon = 10^{-1}$; $N_\varepsilon = 4$, $N_s = 20$, $N_t = \max(100, 5 \times n) = 100$. For deciding the initial values of the parameters, we utilize our former study [32,33,44]. Here, n is the number of decision variables that are to be optimized which is three.

As a result the convergence of the optimum point is reached at the 127th iteration with the optimum values 3.13 m^2, 32.6 m^2, 35.12 kW h of PV area, wind turbine rotor swept area, and battery capacity, respectively. These results led to $33283.6 hybrid energy system total cost. When we compare the result with our former study ($37033.9) [32,33] we obtain a 10.13% improvement on the objective function.

In both studies the results show that the obtained optimum PV area is fairly small relative to wind turbine rotor swept area. This means that the electricity of GSM base station is mostly met by the wind energy. This is probably because of the area's having more potential wind energy rather than solar energy. Besides, the reason may be because the unit cost of photovoltaic is higher than wind energy generator. The amounts of the investment costs that are shared among the four energy sources, PV, wind, battery and auxiliary energy, are seen in Fig. 6. According to this figure, the minimum amount of investment cost belongs to the PV. And, the maximum amount of investment cost belongs to the wind energy source. The battery's and auxiliary energy source's costs are almost same.

RSM consists of a group of mathematical and statistical techniques that can be used to define the relationships between the response and the independent variables. It defines the effect of the independent variables, alone or in combination, on the processes. In addition to analyzing the effects of the independent variables, this experimental methodology also generates a mathematical model called a metamodel. The graphical perspective of the mathematical model has led to the term RSM [45]. In RSM a factorial design is completed first. In other words, the simulation model is run for the experiments of pre-defined input levels. Then, a metamodel, which explains the mathematical relationship between the input and outputs, is estimated from the experiment results. Usually, because the experiments are run for the few levels of inputs the optimization time in RSM is relatively fast. It is a straightforward procedure and easy to apply. However, RSM may not be as efficient as other techniques because the optimization procedure depends on the developed metamodel. In this study, because we utilize our former study to define the initial points and the simulation is run in the DOS environment, the terminating time of the algorithm is reasonable (e.g., <40 min). However, when the number of input increases and/or initial points is defined as far away from the optimum points then the solution time may increase.

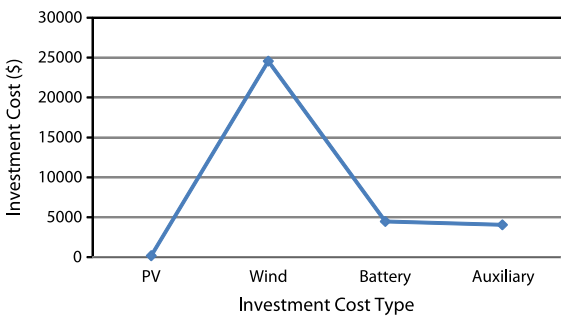

Fig. 6. Investment cost for the GSM base station at the optimum point.

5. Loss of load probability and autonomy analysis

In this paper, the performance of the optimum point of the hybrid system is confirmed in terms of LLP and autonomy analysis on an hourly basis. LLP is defined as, Eq. (9). Here S_j is the total amount of the electricity energy shortage because of not meeting the demand during year j and C_j is the total amount of the electricity energy consumption by GSM base station during year j, and n is the simulation time period, as hour. At the end of the every n year, the LLP is calculated according to Eq. (9). Autonomy is one minus the ratio of the total number of hours in which loss-of-load occurs to the total hours of operation and is given by Eq. (10) [19].

As a result, at the optimum point, the LLP and autonomy curves obtained from the hybrid system simulation are given in Figs. 7 and 8, respectively. According to figures, the LLP value changes between 0.04 and 0.028 and autonomy value changes between 0.92 and 0.855 which can be seen as reasonable. LLP and autonomy values reach their steady state values after some period. If we chose the warm-up period as a longer time period, LLP would reach its steady state value faster than the Figs. 7 and 8. Here, because the unit cost of auxiliary energy is high, the LLP is obtained as small values. If it was taken a smaller value than 0.5, the optimum points so, the LLP would change. Consequently, the optimum sizes which we obtained by the SA is reasonable.

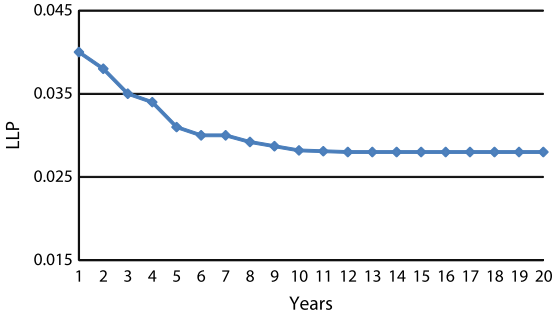

Fig. 7. Yearly LLP values.

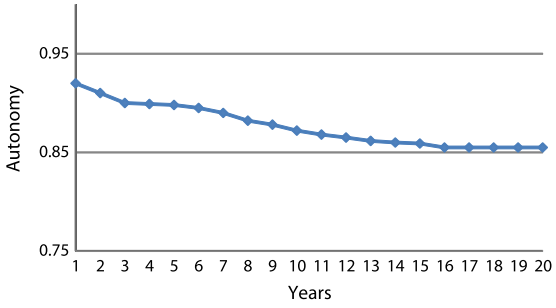

Fig. 8. Yearly autonomy values.

$$LLP = \frac{\sum_{j=0}^{n} S_j}{\sum_{j=0}^{n} C_j} \quad (10)$$

$$A = 1 - \frac{D_{LOL}}{D_{TOT}} \quad (11)$$

6. Conclusions

In this study, we present SA approach for optimizing size of a PV/wind hybrid energy conversion system with battery storage. First, a simulation model representing a detailed hybrid energy system is completed in ARENA 12.0 software. The simulation model is carried out based on the historical hourly mean solar radiation and wind speed data for the period of 2001–2003 recorded at the meteorological station, on a campus area, in Turkey. The input analyzer in ARENA simulation software is used to predict the theoretical distributions of solar radiation, wind speed, and the electricity consumption of the GSM base station inputs in order to run what-if analysis. Second, SA algorithm is used to optimize the model, heuristically. We utilize our former study's result to define the initial values of SA parameters. As a result, the system converges at the 127th iteration with the $33283.6 hybrid energy system total cost. Third the new result is compared with our former study's result and seen that the SA result corresponds to a 10.13% improvement on the objective function. Finally, the performance of the optimum point of the hybrid system obtained by SA is confirmed in terms of LLP and autonomy analysis on an hourly basis. And, consequently the obtained optimum points are assumed to be reasonable.

The methodology described in this study provides an important and systematic approach for design and analysis of hybrid energy systems. This ability is especially helpful if there are various decision variables and large search space to optimize an energy system. Analyzing all possible sizes by simulation is time consuming. Therefore, by using a heuristic approach, SA, we obtain the optimum points at a reasonable time.

The simulation model of this study can be extended in many directions by considering the inflation rate on the unit cost of auxiliary energy and other components. So, the dynamic auxiliary energy unit cost could also affect the optimum total cost and proportion of investment costs. This study is in the process of being extended as a future research with regard to those directions.

References

[1] Sayigh AAM. South–south networking and cooperation on renewable energy and sustainable development. Renew Energy 2004;29(15):2273–5.
[2] Kazmerski LL. Photovoltaics: a review of cell and module technologies. Renew Sustain Energy Rev 1997;1(1–2):71–170.
[3] Asif M, Muneer T. Energy supply, its demand and security issues for developed and emerging economies. Renew Sustain Energy Rev 2007;11(7):1388–413.
[4] Nfah EM, Ngundam JM, Tchinda R. Modeling of solar/diesel/battery hybrid power systems for far-north Cameroon. Renew Energy 2007;32(5):832–44.
[5] Zoulias EI, Lymberopoulas N. Techno-economic analysis of the integration of hydrogen energy technologies in renewable energy-based stand-along power system. Renew Energy 2007;32(4):680–96.
[6] Cai YP, Huang GH, Nie XH, Li YP, Tan Q. Municipal solid waste management under uncertainty: a mixed interval parameter fuzzy–stochastic robust programming approach. Environ Eng Sci 2007;24(3):338–52.
[7] Cai YP, Huang GH, Yang ZF, Lin QG, Bass B, Tan Q. Development of an optimization model for energy systems planning in the region of Waterloo. Int J Energy Res 2008;32(11):988–1005.
[8] Cai YP, Huang GH, Yang ZF, Lin QG, Tan Q. Community-scale renewable energy systems planning under uncertainty-an interval chance-constrained programming approach. Renew Sustain Energy Rev 2009;13(4):721–35.
[9] Sayigh AAM. Renewable energy will meet the challenge in the year 2000. Renew Energy 2000;3(4–5):297–304.
[10] Nfaoui H, Buret J, Sayigh AAM. Stochastic simulation of hourly average wind speed sequences in Tangiers (Morocco). Sol Energy 1996;56(3):301–14.
[11] Nfaoui H, Buret J, Sayigh AAM. Cost of electricity generated and fuel saving of an optimized wind–diesel electricity supply for village in Tangier-area (Morocco). Sol Energy 1996;9(1–4):831–5.
[12] Deepak P, Balachandra P, Ravindranath NH. Grid-connected versus stand-alone energy systems for decentralized power—a review of literature. Renew Sustain Energy Rev, in press.
[13] Hiremath R, Shikha S, Ravindranath N. Decentralized energy planning; modeling and application—a review. Renew Sustain Energy Rev 2007;11(5):729–52.
[14] Diaf S, Notton G, Belhamel M, Haddadi M, Louche A. Design and techno-economical optimization for hybrid PV/wind system under various meteorological conditions. Appl Energy 2008;85(10):968–87.
[15] Borowy BS, Salameh ZM. Methodology for optimally sizing the combination of a battery bank and PV array in a wind–PV hybrid system. IEEE Trans Energy Convers 1996;11(2):367–75.
[16] Markvart T. Sizing of hybrid photovoltaic–wind energy systems. Sol Energy 1996;57(4):277–81.
[17] Yang H, Zhou Wei, Chengzhi Lou. Optimal design and techno-economic analysis of a hybrid solar–wind power generation system. Appl Energy 2009;86(2):163–9.
[18] Celik AN. Optimisation and techno-economic analysis of autonomous photovoltaic–wind hybrid energy systems in comparison to single photovoltaic and wind systems. Energy Convers Manage 2002;43(18):2453–68.
[19] Celik AN. Techno-economic analysis of autonomous PV–wind hybrid energy systems using different sizing methods. Energy Convers Manage 2003;44(12):1951–68.
[20] Morgan TR, Marshall RH, Brinkworth BJ. ARES—a refined simulation programme for the sizing and optimization of autonomous hybrid energy systems. Sol Energy 1997;59(4):205–15.
[21] Yang HX, Lu L, Burnett J. Weather data and probability analysis of hybrid photovoltaic–wind power generation systems in Hongkong. Renewable Energy 2003;28(11):1813–24.
[22] Ashok S. Optimised model for community-based hybrid energy system. Renew Energy 2007;32(7):1155–64.
[23] Bakos GC, Tsagas NF. Technoeconomic assessment of a hybrid solar/wind installation for electrical energy saving. Energy Build 2003;35(2):139–45.
[24] Yang H, Lu L, Zhou W. A novel optimization sizing model for hybrid solar–wind power generation system. Sol Energy 2007;81(1):76–84.
[25] Seeling-Hochmuth GC. A combined optimisation concept for the design and operation strategy of hybrid-PV energy systems. Sol Energy 1997;61(2):77–87.
[26] Bäck T. Evolutionary algorithms in theory and practice. Oxford: Oxford University Press; 1996.
[27] Eiben AE, Smith JE. Introduction to evolutionary computing (natural computing series). Berlin: Springer; 2007.
[28] Bernal-Agustín JL, Dufo-López R. Efficient design of hybrid renewable energy systems using evolutionary algorithms. Energy Convers Manage 2009;50(3):479–89.
[29] Hybrid optimization model for electric renewables (HOMER) 2008. <http://www.nrel.gov/international/homer>.
[30] Dasgupta D, Michalewicz Z. Evolutionary algorithms in engineering applications. Berlin: Springer; 1997.
[31] Bäck T, Fogel DB, Michalewicz Z. Evolutionary computation 1: basic algorithms and operators. Bristol and Philadelphia: Institute of Physics Publishing; 2000.
[32] Ekren O, Ekren BY. Size optimization of a PV/wind hybrid energy conversion system with battery storage using response surface methodology. Appl Energy 2008;85(11):1086–101.
[33] Ekren O, Ekren BY. Break-even analysis and size optimization of a PV/wind hybrid energy conversion system with battery storage – a case study. Appl Energy 2009;86(7–8):1043–54.
[34] Kelton WD, Sadowski RP, Sturrock DT. Simulation with arena. 3rd ed. New York: McGrawHill; 2004.
[35] Kleijnen JPC. Statistical tools for simulation practitioners. 1st ed. New York: Marcel Dekker; 1987.
[36] Ekren O. Optimization of a hybrid combination of a photovoltaic system and a wind energy conversion system. M.S. Thesis. Department of Mechanical Engineering. Izmir Institute of Technology, Turkey; 2003.
[37] Klein SA. Calculation of monthly average insolation on tilted surfaces. Sol Energy 1977;19(4):325–9.
[38] Muselli M, Notton G, Louche A. Design of hybrid photovoltaic power generator with optimization of energy management. Sol Energy 1999;65(3):143–57.
[39] Kemmoku Y, Egami T, Hiramatsu M, Miyazaki Y, Araki K, Ekins-Daukes NJ, et al. Modelling of module temperature of a concentrator PV system. In: Proc. 19th European photovoltaic solar energy conference; 2004. p. 2568–71.
[40] Kirkpatrick S, Gelatt CD, Vecchi MP. Optimization by simulated annealing. Science 1983;220(4598):671–80.
[41] van Laarhoven PJM, Aarts EHL. Simulated annealing: theory and applications. Dordrecht: Reidel; 1987.
[42] Aarts EHL, Korst JHM, van Laarhoven PJM. Simulated annealing. In: Aarts E, Lenstra J, editors. Local search in combinatorial optimization. Chichester: Wiley; 1997. p. 91–120.
[43] Metropolis N, Rosenbluth AW, Rosenbluth MN, Teller AH, Teller E. Equations of state calculations by fast computing machines. J Chem Phys 1953;21:1087–92.
[44] Goffe WL, Ferrier GD, Rogers J. Global optimization and statistical functions with simulated annealing. J Econom 1994;60(1–2):65–99.
[45] Box GEP, Draper NR. Empirical model-building and response surfaces. 1st ed. New York: John Wiley & Sons; 1987.